Solid Freeform Fabrication 2023: Proceedings of the 34th Annual International Solid Freeform Fabrication Symposium – An Additive Manufacturing Conference
Reviewed Paper

A Comparison of Microstructure and Mechanical Performance of Inconel 718 Manufactured via L-PBF, LP-DED, and WAAM Technologies

Nabeel Ahmad[1,2], Alireza Bidar[1,2], Reza Ghiaasiaan[1,2], Paul R. Gradl[3], Shuai Shao[1,2], Nima Shamsaei[1,2*]

[1] National Center for Additive Manufacturing Excellence (NCAME), Auburn University, Auburn, AL 36849, USA

[2] Department of Mechanical Engineering, Auburn University, Auburn, AL36849, USA

[3] NASA Marshall Space Flight Center, Propulsion Department, Huntsville, AL 35812, USA

*Corresponding author: shamsaei@auburn.edu

Phone: (334) 844-4839

Abstract

The microstructure and mechanical properties of additively manufactured (AM) alloys can be significantly affected by variations in cooling rates, resulting from different process conditions across different additive manufacturing (AM) platforms. Therefore, it is crucial to understand the effect of manufacturing process on the microstructure and mechanical properties of AM Inconel 718. This study examines three AM processes: laser powder bed fusion, laser powder directed energy deposition, and wire arc additive manufacturing. Results show that fully heat treated laser powder bed fused (L-PBF) and wire arc additively manufactured (WAAM) Inconel 718 specimens exhibit higher strength compared to laser powder directed energy deposited (LP-DED) ones due to finer grain structure in L-PBF and retained dendritic microstructure in WAAM. The ductility in LP-DED Inconel 718 was slightly higher compared to WAAM and L-PBF due to relatively small carbide size, which causes stress concentration in a small material volume, leading to delayed fracture.

Keywords: Additive manufacturing (AM); Laser powder bed fusion (L-PBF); Laser powder directed energy deposition (LP-DED); Wire arc additive manufacturing process (WAAM); Inconel 718

Introduction

Additive manufacturing (AM) offers several advantages over traditional manufacturing such as design flexibility, the ability to fabricate complex geometries, and the capability to manufacture hard-to-machine materials such as Inconel 718 [1]. Different AM technologies have been developed, with laser powder bed fusion (L-PBF), laser powder directed energy deposition (LP-DED), and wire arc additive manufacturing (WAAM) being the most commonly used [2]. Each of these technologies has its unique benefits and limitations. For instance, LP-DED and WAAM processes have higher throughput than L-PBF and suitable for larger part sizes, but they have lower accuracy and may not be ideal for intricate features [3].

Despite numerous advantages, qualifying and certifying AM parts remain challenging due to the inherent variability in mechanical performance caused by unique micro-/defect- structures. This issue is compounded by differences in cooling rates among technologies, resulting from variations in process parameters, feedstock size, and mass deposition or layer thickness [4,5]. Varied cooling rates have a significant impact on microstructure and mechanical properties [6]. Moreover, the microstructural response to standard heat treatment (HT) can vary significantly across different AM processes [7]. While previous studies have mainly investigated the effects of individual AM processes on microstructure and mechanical properties [8,9], very few have directly compared multiple technologies in terms of microstructural response to standard HT and resulting mechanical properties [3,10]. This study aims to provide a direct comparison of the microstructure and mechanical properties of Inconel 718 manufactured via three commonly used technologies: L-PBF, LP-DED, and WAAM.

Experimental Procedure

The cylindrical bars of Inconel 718 were fabricated using L-PBF, LP-DED, and WAAM technologies. The chemical composition of powder used in this study for fabrication of L-PBF and LP-DED specimens is exhibited in **Table 1**. The process parameters employed in L-PBF and LP-DED machines are shown in **Table 2**. Note that the process parameters employed in WAAM machine were proprietary and not shown in this article. After fabrication, the specimens in all the manufacturing conditions underwent multi-step HT. This involved stress relief (SR) at 1066°C for 1.5 hr, followed by the hot isostatic pressing (HIP) at 1162°C at 103 MPa for 3 hr, then solution annealing (SA) at 1065°C for 1 hr. Lastly, double aging (DA) which consisted of first step at 760°C for 10 hrs and second step at 650°C for 10 hrs. A schematic illustration of the followed HT is also shown in **Figure 1**. Following HT, the specimens were machined to the tensile geometry, which had dimensions according to ASTM E8 standard [11] (see **Figure 2**).

For microstructure analysis, small coupons were cut from the tensile specimens and then mounted in cold epoxy resin. These samples were prepared for scanning electron microscopy (SEM) using a semi-automatic mechanical polisher. The samples were initially ground using sandpapers, then polished on ChemoMet, and finally underwent vibratory finishing to remove any residual layers resulting from grinding or polishing. Microstructure analysis was performed using a Zeiss Crossbeam scanning electron microscope (SEM), equipped with electron backscatter diffraction and energy-dispersive X-ray spectroscopy detectors.

Table 1 Chemical compositions (Wt.%) of powders used in this study.

Elements	**L-PBF**	**LP-DED**
C	0.03	0.04
Mn	0.08	0.11
Si	0.09	0.06
S	<0.015	<0.001
P	0.01	0.01
Cr	18.09	18.81
Fe	18.33	Bal
Co	0.35	<0.1
Mo	2.91	3.01
Nb+Ta	5.00	5.18
Ti	0.95	0.96
Al	0.38	0.52
B	<0.006	0.00
Cu	0.04	0.02
Ca	<0.01	-
Mg	<0.01	-
O	0.01	0.01
N	0.03	<0.001
Se	<0.005	
Ni	53.60	52.69

Table 2 The process parameters used for manufacturing of Inconel 718 tensile specimens via L-PBF and LP-DED technologies.

Process	Power (W)	Layer thickness (mm)	Travel speed (mm/s)	Powder feed rate (g/s)
L-PBF	285	0.04	960	---
LP-DED	1070	0.381	16.93	0.26

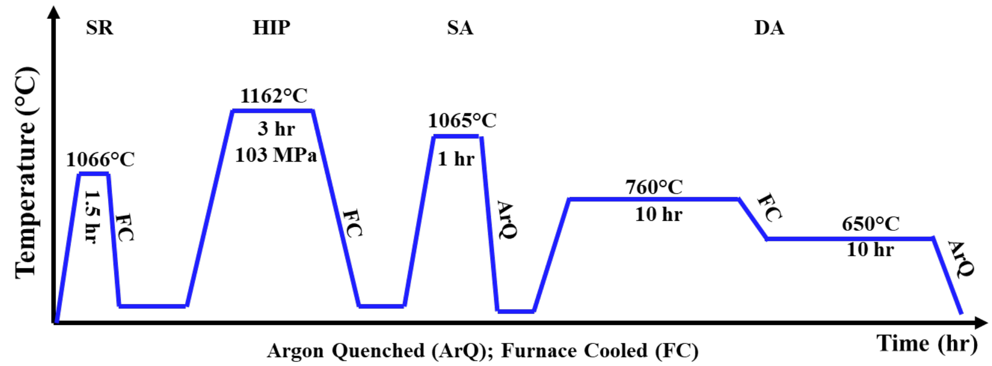

Figure 1 Schematic illustration of multi-step HT followed in this study.

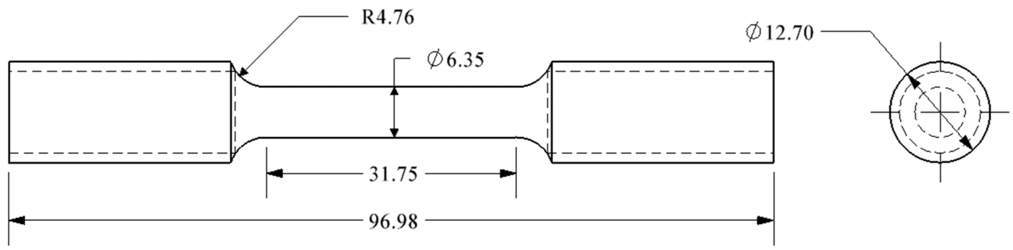

Figure 2 The geometry of the tensile specimen used in this study. All dimensions are in mm.

Results and Discussion

The inverse pole figure (IPF) maps obtained from both non-heat-treated (NHT) and heat treated (HT) conditions of laser powder bed fused (L-PBF), wire arc additively manufactured (WAAM), and laser powder directed energy deposited (LP-DED) samples are presented in **Figure 3.** In NHT condition, L-PBF Inconel 718 samples exhibited finer grain structure (see **Figure 3(a)**), which is attributed to their high cooling rates [3]. The grain size distribution revealed that all grains in L-PBF samples were smaller than 100 µm (**Figure 3(g)**), whereas LP-DED and WAAM samples had predominantly larger grains exceeding 200 µm. After full HT, L-PBF and LP-DED conditions exhibited recrystallization and subsequent grain growth, while WAAM samples retained the as-fabricated characteristics. Moreover, the annealing twins were also observed in LP-DED and L-PBF samples, but not in WAAM ones, further validating that recrystallization did not occur in WAAM samples. The grain size distribution of the HT samples showed that the majority of grains in L-PBF specimens were below 200 µm, while LP-DED and WAAM samples predominantly had grains larger than 300 µm (see **Figure 3(h)**).

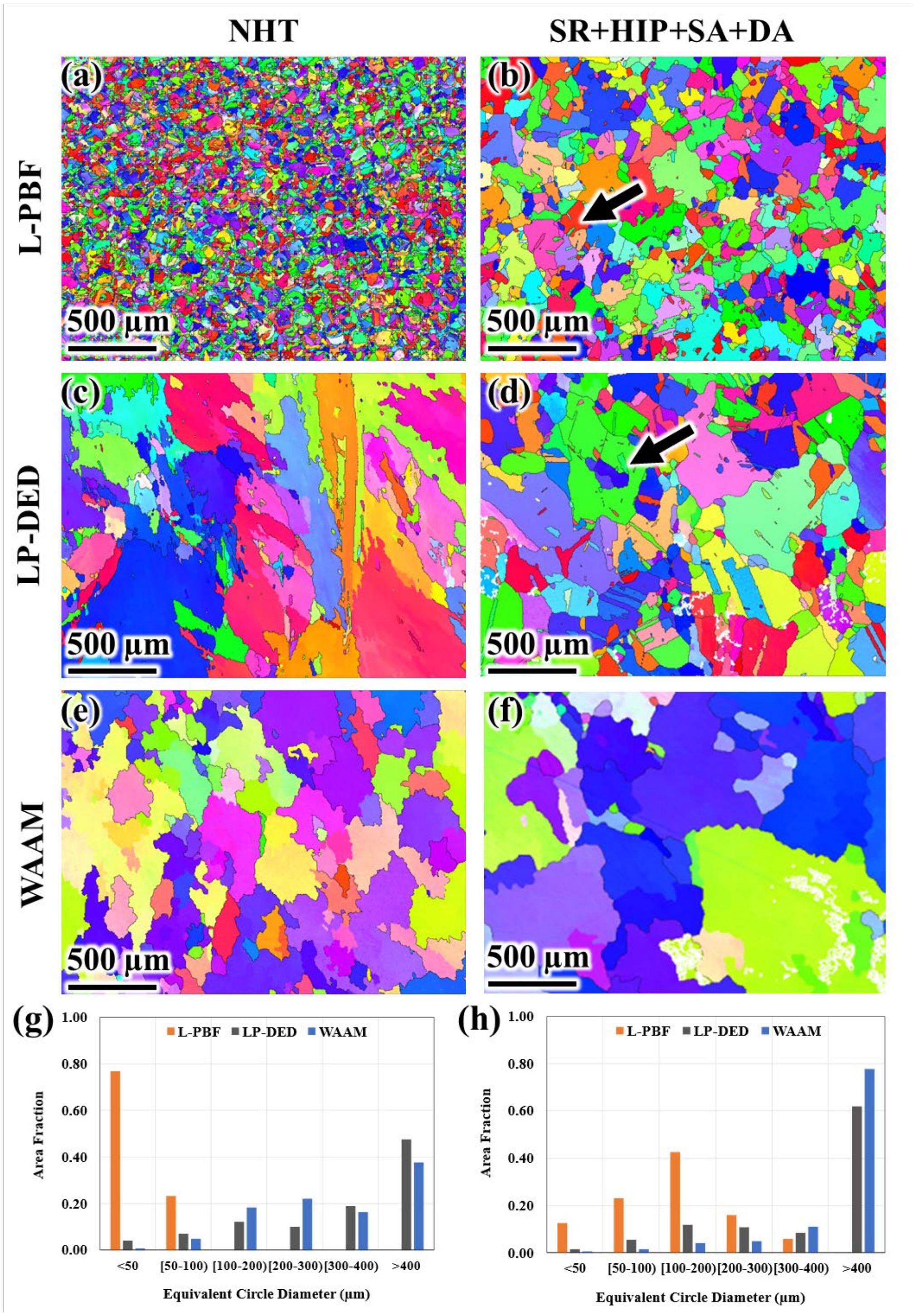

Figure 3 The IPF maps obtained from L-PBF, LP-DED, and WAAM samples in different HT conditions. (g) and (h) exhibit the grain size distribution in NHT and HT conditions, respectively. The black arrows indicate annealing twins.

The BSE images obtained from the radial plane (i.e., the plane perpendicular to build direction) of NHT and fully HT specimens in all the processing conditions are presented in **Figure 4**. The NHT microstructure in all processing conditions exhibited dendritic microstructure, with finer dendrites observed in L-PBF compared to LP-DED and WAAM samples. Upon full HT, the dendritic characteristics were dissolved in both LP-DED and L-PBF specimens, while WAAM specimens retained the dendritic microstructure. The bright particles within grains and at the grain boundaries are likely Mo-rich carbides, as described in previous studies [12,13]. The size of M_6C carbides appeared to be larger in L-PBF and WAAM samples than in LP-DED samples (see insets of **Figures 4(b), (d), and (f)**). Moreover, the volume fraction of carbides in WAAM appeared to be higher than LP-DED and L-PBF samples.

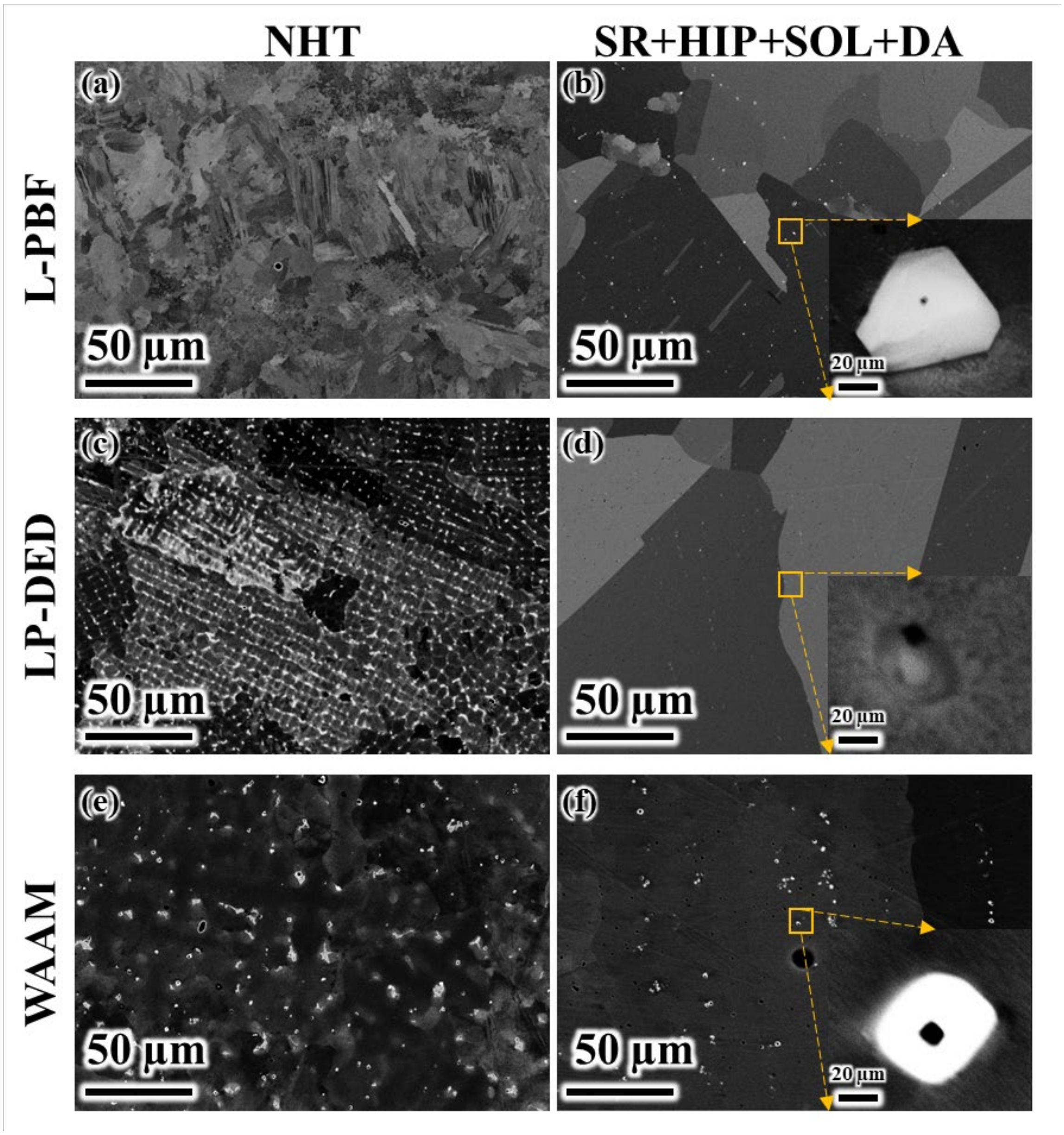

Figure 4 The BSE images obtained from the radial plane of NHT and HT samples in different processing conditions.

The tensile properties including yield strength (YS), ultimate tensile strength (UTS), and elongation to failure (EL) are presented in **Figure 5** for L-PBF, LP-DED, and WAAM Inconel 718 specimens. Moreover, these properties are compared with those of electron powder bed fused (E-PBF) [9] and wrought counterparts [14]. Interestingly, the wrought parts showed similar strengths and EL to L-PBF and WAAM specimens. Moreover, the YS and UTS of L-PBF and WAAM specimens were higher compared to LP-DED and E-PBF, while EL was slightly lower compared to LP-DED and E-PBF. The difference in strength can be attributed to the finer grain structure in L-PBF and retained as-fabricated characteristics in WAAM. Finer grain size and dendritic microstructures limit dislocation pileup, leading to higher strengths according to Hall-Petch strengthening [15,16]. The higher EL of LP-DED specimens compared to WAAM and L-PBF can be attributed to the smaller size of carbides in LP-DED, which impose stress concentration on smaller material volume. Therefore it is more difficult for smaller carbide to debond from matrix [13]. The tensile fracture surfaces of L-PBF and LP-DED Inconel 718 are shown in **Figure 6,** exhibiting typical cup and cone fractures with a fibrous region in the center and shear lips around the periphery. Higher magnification images revealed finer dimples in L-PBF specimens, while LP-DED specimens exhibit larger dimples, indicating delayed fracture. The carbide particles were also observed inside the dimples, validating that carbide debonding governed the fracture behavior in all specimens, regardless of the manufacturing process.

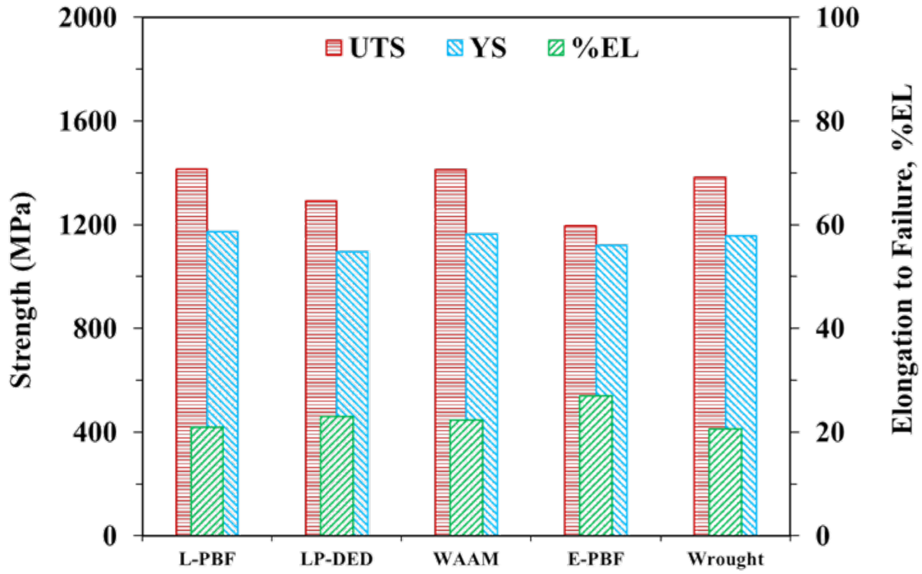

Figure 5 Tensile properties of fully HT and machined L-PBF, LP-DED, WAAM, E-PBF and wrought Inconel 718 specimens.

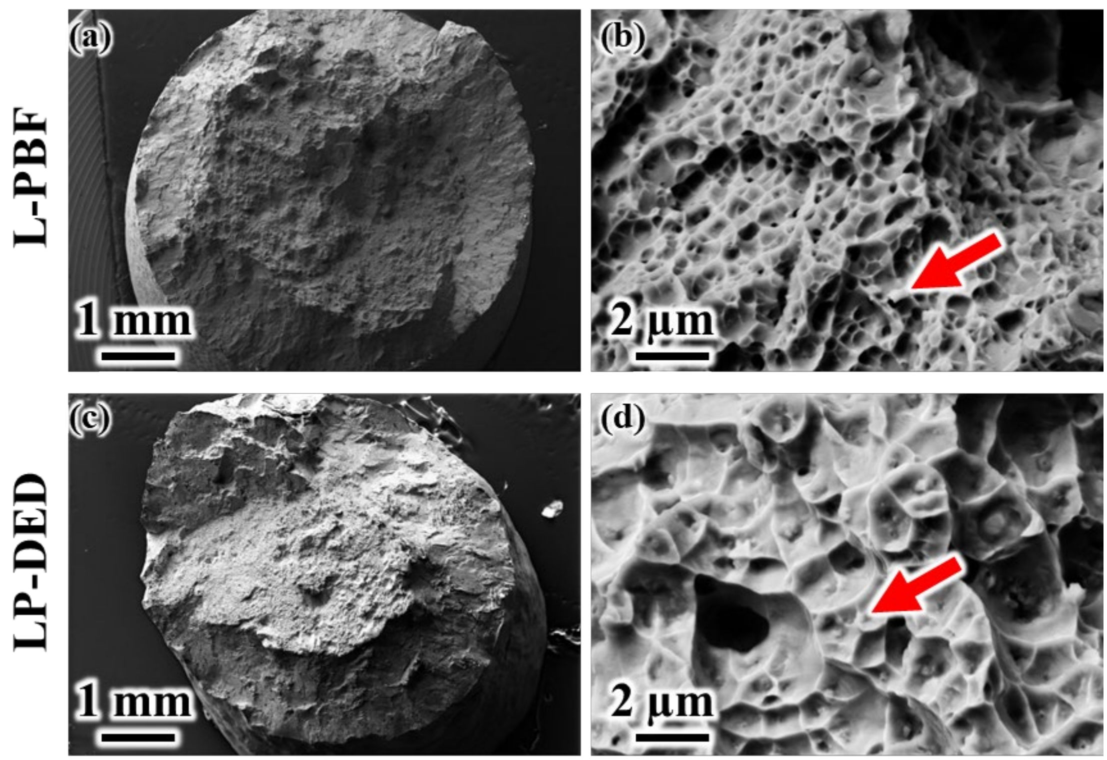

Figure 6 The fracture surfaces of (a)-(b) L-PBF and (c)-(d) LP-DED Inconel 718 specimens. Red arrows indicate fractured particles.

Conclusions

This study investigated the effect of additive manufacturing process on the microstructure and tensile properties of Inconel 718. The specimens were fabricated using laser powder bed fusion, laser powder directed energy deposition, and wire arc additive manufacturing. All specimens underwent an identical heat treatment schedule. The tensile properties generated from this study are compared with those of the wrought and electron powder bed fused counterparts. The following conclusions are drawn from this study:

1) The non-heat treated microstructure exhibited dendritic microstructure regardless of the manufacturing condition. Moreover, the size of the grains in laser powder bed fused (L-PBF) Inconel 718 samples was finer compared to laser powder directed energy deposited (LP-DED) and wire arc additively manufactured (WAAM) Inconel 718 ones.
2) Upon full heat treatment, dendritic characteristics were not observed in L-PBF and LP-DED samples, while it was observed in WAAM samples. Moreover, the fully heat treated samples in L-PBF and LP-DED conditions exhibited recrystallization and significant grain growth.
3) The grain size of L-PBF Inconel 718 in the fully heat treated condition was finer compared to LP-DED and WAAM ones.
4) The fully heat treated and machined specimen in L-PBF and WAAM conditions exhibited higher strength compared to those of LP-DED and electron powder bed fused ones due to finer grain structure in the former and dendritic microstructure in the latter.
5) The elongation to failure of LP-DED specimens was slightly higher than WAAM and L-PBF specimens due to smaller carbide particles causing stress concentration in a smaller volume, resulting in delayed microvoid coalescence and fracture.

Acknowledgment

This research is partially supported by the National Aeronautics and Space Administration (NASA) under Cooperative Agreement No. 80MSFC19C0010. This paper describes objective technical results and analysis. Any subjective views or opinions that might be expressed in the paper do not necessarily represent the views of the NASA or the United States Government.

References

[1] A. Yadollahi, N. Shamsaei, Additive manufacturing of fatigue resistant materials: Challenges and opportunities, Int. J. Fatigue. 98 (2017) 14–31.

[2] T. DebRoy, H.L. Wei, J.S. Zuback, T. Mukherjee, J.W. Elmer, J.O. Milewski, A.M. Beese, A. Wilson-Heid, A. De, W. Zhang, Additive manufacturing of metallic components – Process, structure and properties, Prog. Mater. Sci. 92 (2018) 112–224.

[3] P.D. Nezhadfar, P.R. Gradl, S. Shao, N. Shamsaei, Microstructure and Deformation Behavior of Additively Manufactured 17–4 Stainless Steel: Laser Powder Bed Fusion vs. Laser Powder Directed Energy Deposition, Jom. 74 (2022) 1136–1148.

[4] R. Shrestha, N. Shamsaei, M. Seifi, N. Phan, An investigation into specimen property to part performance relationships for laser beam powder bed fusion additive manufacturing, Addit. Manuf. 29 (2019).

[5] A. Soltani-Tehrani, R. Shrestha, N. Phan, M. Seifi, N. Shamsaei, Establishing specimen property to part performance relationships for laser beam powder bed fusion additive manufacturing, Int. J. Fatigue. 151 (2021) 106384.

[6] A. Yadollahi, N. Shamsaei, S.M. Thompson, D.W. Seely, Effects of process time interval and heat treatment on the mechanical and microstructural properties of direct laser deposited 316L stainless steel, Mater. Sci. Eng. A. (2015).

[7] J. Schneider, Comparison of Microstructural Response to Heat Treatment of Inconel 718 Prepared by Three Different Metal Additive Manufacturing Processes, Jom. 72 (2020) 1085–1091.

[8] T. Trosch, J. Strößner, R. Völkl, U. Glatzel, Microstructure and mechanical properties of selective laser melted Inconel 718 compared to forging and casting, Mater. Lett. 164 (2016) 428–431.

[9] D. Deng, Additively Manufactured Inconel 718 : Microstructures and Mechanical Properties, 2018.

[10] M. Muhammad, R. Gusain, S. Reza Ghiaasiaan, P.R. Gradl, S. Shao, N. Shamsaei, Microstructure and mechanical properties of additively manufactured Haynes 230: A comparative study of L-PBF vs. LP-DED, 2022 Int. Solid Free. Fabr. Symp. (2022).

[11] ASTM E8, ASTM E8/E8M standard test methods for tension testing of metallic materials 1, Annu. B. ASTM Stand. 4. (2010) 1–27.

[12] N. Ahmad, S. Baig, S. Reza Ghiaasiaan, P.R. Gradl, S. Shao, N. Shamsaei, Microstructure and mechanical properties of additively manufactured Inconel 718: A comparative study between L-PBF and LP-DED, (2022).

[13] N. Ahmad, R. Ghiaasiaan, P.R. Gradl, S. Shao, N. Shamsaei, Revealing deformation mechanisms in additively manufactured Alloy 718: Cryogenic to elevated temperatures, Mater. Sci. Eng. A. 849 (2022) 143528.

[14] Haynes International, IN 718, (n.d.).

[15] N. Ahmad, S. Shao, M. Seifi, N. Shamsaei, Additively manufactured IN718 in thin wall and narrow flow channel geometries: Effects of post-processing and wall thickness on tensile and fatigue behaviors, Addit. Manuf. 60 (2022) 103264.

[16] T.G. Gallmeyer, S. Moorthy, B.B. Kappes, M.J. Mills, B. Amin-Ahmadi, A.P. Stebner, Knowledge of process-structure-property relationships to engineer better heat treatments for laser powder bed fusion additive manufactured Inconel 718, Addit. Manuf. 31 (2020) 100977.